

**How to Cite:**

Akinluyi, F. O. (2022). Enhancing geostatistical prediction of total hydrocarbon content (THC) using Bayesian maximum entropy (BME) in a region of Niger Delta, Nigeria. *International Journal of Health Sciences*, 6(S6), 826–838.  
<https://doi.org/10.53730/ijhs.v6nS6.9679>

## **Enhancing geostatistical prediction of total hydrocarbon content (THC) using Bayesian maximum entropy (BME) in a region of Niger Delta, Nigeria**

**F. O. Akinluyi**

Department of Remote Sensing and GIS, the Federal University of Technology, Akure, Nigeria

Email: [foakinluyi@futa.edu.ng](mailto:foakinluyi@futa.edu.ng)

Orchid: 0000-0002-1390-1831

**Abstract**---In this study, Bayesian maximum entropy (BME) was implemented to take advantage of the limited data available for reliable prediction of total hydrocarbon content (THC) in the soil because it allows assimilate of secondary and its uncertainty data. Thirteen (13) physico-chemical soil variables were obtained. Upon the application of multiple regression analysis to the soil variables, electrical conductivity, EC was found as a covariate to the eleven (11) [THC] \_hard data. Twenty-eight (28) [THC] \_(soft ) data were then generated by regression model between [THC] \_hard and EC and their 28 uncertainty data were also derived using probability density function. Therefore, 11 [THC] \_hard, 28 [THC] \_(soft )and 28 error data in the computation of THC soft were integrated at BME technique to produce BME prediction and BME standard deviation maps of THC. The BME predicted THC value in the area ranges from 0 – 16 mg/kg. The BME prediction map provides the mean variable of the estimation posterior pdf of THC. It shows the spatial variability of THC as the concentration decreases from the highest concentrated zone of THC. This is a point source spillage and may be due to vandalization of oil-well heads and flowlines, operational failure, surface or underground pipeline leakages due corrosion effect or obsolete equipment just to mention a few. The THC guide value for normal soil is 100 mg/kg. The BME standard deviation provides measure of the accuracy assessment in the BME prediction of THC. The BME standard deviation map varies between 1 and 8 mg/kg. The BME standard deviation is highest at the region where BME prediction is highest. The high BME estimation standard deviation is attributed to the weak correlation between THC and EC used to generate the [THC] \_soft and inclusion of its measurement error in the BME prediction of THC. This

study demonstrates the usefulness of BME method having solid theoretical foundation and its computational ability to systematically process soft data coming from regression model and its uncertainty.

**Keywords**---Niger Delta Region, hydrocarbon spillage, total hydrocarbon content (THC), electrical conductivity (EC), bayesian maximum entropy (BME).

## **Introduction**

Hydrocarbon spillage is a global issue that has been occurring since the discovery of crude oil, which was part of the industrial revolution. The first oil well in Nigeria was discovered in 1956 at Oloibiri in the present day Bayelsa state by Royal Dutch Shell and commercial production began in 1958 (Kellett, 1990; Oguine, 1999; Elum et al., 2016; Ukhurebor et al., 2021). Ever since this discovery, there have been continuous exploration and exploitation activities going-on in the oil producing province of Niger Delta, Nigeria. Although, oil industry has contributed immensely to the growth and development of the country but unsustainable crude oil exploration activities have rendered the Niger Delta region one of the most severely damaged ecosystems in the world (Olaseni and Alade, 2012; Ukhurebor et al., 2021). As such, hydrocarbon oil spillage is an unavoidable consequence of industrialisation and economic development which has caused a considerable loss of mangroves and arable agricultural lands.

An oil spillage is the discharge of hydrocarbon products into terrestrial or marine ecosystem. Serious dilapidation ensuing from the economic activities of various companies and agencies in the petroleum sector has been discovered to exhibit deleterious environmental implications. However, terrestrial spills may arise from activities of saboteur/vandals to well heads and flowlines, obsolete/malfunctioning equipment, underground and surface pipeline leakages, oil well blow-out due to overpressure, accidental discharge/hose failure, failed pipelines due to corrosion effect and operational failure, as well as transport of oil slicks from sea to land (Awobajo, 1981; Okpokwasilli and Amanchukwu, 1988; Kadafa, 2012; Ukhurebor et al., 2021). Some of these modes of oil spillage occurrence usually cause serious destruction to the environment thereby putting the lives, property and means of livelihood of the people who are predominantly farmers and fisher men in great jeopardy. The devastating consequences of the spillage are enormous in the region on both aerial and terrestrial environments to a complex chain effect on both the bio-diversity and human health. In recent time, concern about the region and its future has triggered negative effects in the affected communities with reduced source of livelihood, and no level of clean up can restore the soil fertility. The United Nation Environmental Programme (UNEP, 2011) discovered that residents in the Niger Delta region are vulnerable to elevated levels of hydrocarbon in contaminated drinking water and outdoor air which posed a dangerous threat to their health and welfare.

Investigation of hydrocarbon polluted soils often involves direct sampling of soils and water (i.e., both surface and underground) from mechanically drilled shallow/deep boreholes or pits and subsequent physical and chemical analysis

(Echefu and Akpofure, 2002; Akinlo, 2012). Many boreholes or pits are required for reasonable accurate delineation of both the vertical and the lateral extent of the pollution plume. Hence, the cost of quantifying the plume is high while the duration of such investigation is considerably long (Akpan, 2010; Olaseni and Alade, 2012; Adetunji and Ukhurebor, 2021). In addition to this limitation, direct investigation method lacks continuity as information obtained has the support of single with respect to particular sampling points. However, application of modern geostatistics (i.e., Bayesian Maximum Entropy, BME) is used in this study within the framework of reliable spatial estimator (Christakos, 1990; Christakos and Li, 1998; Christakos, 2000; Christakos et al., 2004) whereby the classical geostatistics, mainly including the various kriging techniques (Cressie and Hawkins, 1980; Lark, 2000) are considered as special cases. The essence of applying BME rather than traditional geostatistics is because the latter is less sensitive to outliers (Christakos, 1990; Christakos and Li, 1998; Shi et al., 2015) in quantify the spatial attributes of a phenomenon than the former. The existence of outliers will greatly affect the variogram form and cause erratic behaviour of the variogram model. A point source spillage in the case of hydrocarbon pollution may be seen as an outlier that probably carry critical information that should be process carefully and, in this instance, should not be removed which is a usual practice in data analysis process (Zhang et al., 2009; Zhang and Yang, 2019).

Bayesian maximum entropy (BME) (Christakos, 1990; 1992) is an innovative prediction technique amongst the suites of geostatistical methods. It provides a systematics and rigorous method for incorporating various physical knowledge bases (denoted as KB) into the analysis and mapping of natural variables soft data and other sources of information. Actually, BME can take the space/time variability structure model into account, together with the possibility of using interpretative and soft information, besides the hard data. Douaik et al. (2005) employed the spatio-temporal kriging and BME to delineate soil salinity by integrating interval-type soft as well as hard data in soil salinity mapping in the Hortobagy National Park, Hungary. Improved performance of BME was stated against kriging. Modis et al. (2010) studied the ammonium hydrogeological contamination and its uncertainty using BME framework in Greek lignite region. Zhang and Yang (2019) used the BME technique by converting outliers into soft data so as to improve the predictions of the soil Zn contents in the Wuhan city in the central China. Rezaei et al., 2020 improved geostatistical predictions of two soil variables by using Bayesian maximum entropy in a mining site at Sungun.

Mismanagement of the oil and gas industry over the decades in the Niger Delta has caused huge amount of land water, and air pollution. The focus of this study is on land pollution through the primary measurement of total hydrocarbon content (THC) and other soil variables. THC is a soil chemical property for evaluating the quantity of the measured hydrocarbon impurities present. The aim of this study is to determine a covariate to generate soft data and include its uncertainty in the prediction process of THC using BME technique. Environmental pollution assessment using BME is a valuable tool for environmental evaluation of earth systems, in particular soils. It is reliable estimator that accommodate others

## Materials and Methods

### Study Area

The study area is located in the Niger Delta. It is one of the numerous on-shore oil-well flow stations in the oil province region of Nigeria called Niger Delta. The Niger Delta is a large area of southern Nigeria. It is home to around 30 million people comprising Rivers, Bayelsa, Delta, Akwa Ibom, Cross River, Edo, Abia, Imo and Ondo State. The Niger Delta is biodiverse, with its mangroves providing carbon sequestration capacity and supporting a wide variety of plant and animal life, as well as the agriculture and fishing on which many in the region rely for their livelihoods.

### Data Preparation

Results of thirteen (13) physico-chemical soil variables were obtained to undertake this study. The data set are sand, silt, clay, total hydrocarbon content (THC), and electrical conductivity (EC). These data were subjected to multiple regression analysis whereby sand, silt, clay, electrical conductivity (EC), phenol, chromium (Cr), lead (Pb), nickel (Ni), iron (Fe), sulphates (SO<sub>4</sub>), phosphates (PO<sub>4</sub>), chlorine (Cl) are designated as predictor variables and total hydrocarbon content (THC) hard data as a response variable. The essence of this is to determine a covariate that can predict THC because the eleven (11) THC hard data is not sufficient to make a reliable prediction. The spatial distribution of eleven THC hard data points overlay on Google Earth image is shown in Figure 1. Thus, regression model, equation (1) of the form:

$$\begin{aligned} THC_{soft}(hs) &= \beta_0 + \beta_1 * EC & (1a) \\ THC_{soft}(hs) &= 0.0432 * (EC) - 0.4587 & (1b) \end{aligned}$$

was built to generate  $THC_{soft}(hs)$  data. Where  $\beta_0$  and  $\beta_1$  are constants equivalent to -0.4587 and 0.0432 respectively. The regression model of equation (1b) is shown in Figure 2 such that the correlation coefficient,  $C.C. = 0.62$  occurred between THC and EC. Hence, twenty-eight (28)  $THC_{soft}$  data were generated using equation 1b. Figure 3 shows the distribution of 28  $THC_{soft}$  data overlay on Google Earth image. The variance at each point where an observation of  $EC$  was made was computed using equation 2:

$$s^2 = \{(x_0^T (X^T X)^{-1} x_0 + 1) * MSE\} \quad (2)$$

Where  $x_0$  = vector of EC value,  $x_0^T$  = transpose of  $x_0$ ,  $(X^T X)^{-1}$  = inverse of 2x2 matrices of EC values, MSE = mean square of the residual, and  $s^2$  = variance of the prediction error. Therefore, the uncertainty  $THC_{error}$  in the computation of  $THC_{soft}$  data was derived by using probability density function (PDF), represented by equation 3:

$$g(hs) = \frac{1}{s\sqrt{2\pi}} e^{-\left(\frac{(hs-\bar{hs})^2}{2s^2}\right)} \quad (3)$$

Where  $g(hs)$  = normal density function at 95% confidence interval,  $hs$  = soft data, and  $\overline{hs}$  = mean value of the soft data.

Finally, the initial 11  $THC_{hard}$  data is now enlarged to a total of thirty-nine (39) THC data comprising 11  $THC_{hard}$  and 28  $THC_{soft}$  data. 28  $THC_{error}$  computation error is also available



Figure 1. 11  $THC_{hard}$  data overlay on Google Earth Image

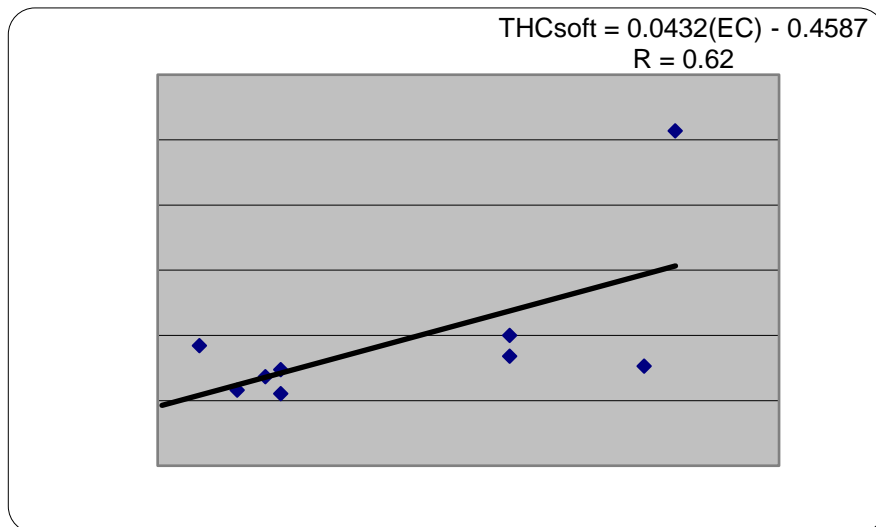


Figure 2. Linear regression graph between THC and EC

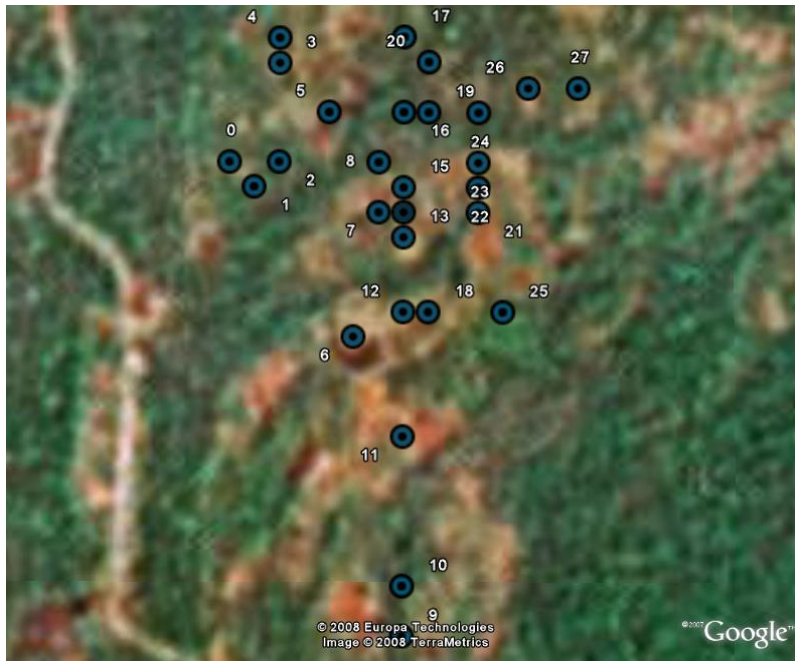


Figure 3. 28  $THC_{soft}$  data overlay on Google Earth Image

for integration by a reliable spatial estimator called Bayesian maximum entropy (BME). The combination of all these data was referred to as THC in results and discussion.

### **Spatial Prediction Bayesian Maximum Entropy (BME)**

The concept of BME approach to spatial estimation is the combination of three interrelated stages. They are general knowledge, site specific and integration (posterior) stage. BME has the capability of assimilating hard, soft and measurement error data into geospatial prediction process in which kriging and other interpolation techniques lack, and are seen as special case of BME (Christakos and Li, 1998; Christakos, 1990; Christakos, 2000). The three stages of the BME framework are as follows:

#### **General knowledge stage (G)**

According to BME framework, the first task is to carry out what is called general knowledge base of the study. This stage is relative to prior knowledge. The mean and covariance components of general knowledge base were determined i.e., spatial correlation modelling. For geostatistical applications, the general knowledge (G) was transformed to mean trend and covariance. The spatial estimation process operates on de-trended data. The log-transformed data is given by:

$$Y_{data} = \log(Z_{data}) \quad (4)$$

The mean trend function was obtained by smoothing the logarithmic data  $Y_{data}$ . This mean trend represents the systematic trend in the spatial distribution of  $THC_{hard}$  data across the study area. Using the log-transformed data  $Y_{data}$  and the mean trend model  $m_y(s)$  described above, the data for the residual,  $X_{data} = Y_{data} - m_{ydata}$  was obtained to calculate the covariance,  $c_{xm}(r)$ . The covariance is given by:

$$(5) \quad c_{xm}(r) = c \exp\left\{-3\frac{r}{a}\right\}$$

Exponential function was used to fit the covariance model in equation (5). Where  $c$  is the sill value,  $a$  is the range and  $r$  is the spatial lag. Trend was removed by employing kernel filter. Hence, the prior PDF  $f_G$  obtained is multivariate Gaussian, i.e.

$$(6) \quad f_G(u_{map}, s_{map}) = \varphi(u_{map}; m_{map}, c_{map})$$

providing initial probability distributions across space. Where  $u_{map}$  is a vector of values of hard and soft data at the mapping points,  $s_{map}$  is the spatial coordinates of these mapping points,  $m_{map}$  is the vector of mean trend values provided by the mean trend model at the mapping points,  $c_{map}$  is a matrix of covariance provided by the covariance model for all pairs of mapping points, and  $\varphi$  is the multivariate Gaussian PDF (Serre and Christakos, 1999).

### Site specific stage (S)

It is a stage about a specific situation where data are organised. A particular occurrence or state of affairs at a particular location and at a particular time. The available knowledge base (G) for the site-specific stage (S) consists of hard and soft data:

- Hard data: these are measured data (i.e., primary data) obtained from the sample location where hydrocarbon spillage had occurred.
- Soft data: these are secondary data obtained from regression model. It is considered as an additional data to complement the few THC data available.

The mapping points  $u_{map}$  include both the data points  $u_{data}$  and the estimation point  $hp(s_k)$  i.e.,  $u_{map} = \{u_{data}, hp(s_k)\}$ .

$$\text{Hard data, } ht(s_i) = \{ht_1, ht_2, \dots, ht_{11}\} \quad (7)$$

$$\text{Spatial location of hard data, } s_i = \{s_1, s_2, \dots, s_{11}\} = T_1 \quad (8)$$

$$\text{Soft hard, } hs_j = \{hs_1, hs_2, \dots, hs_{28}\} \quad (9)$$

$$\text{Spatial location with soft data, } s_j = \{s_1, s_2, \dots, s_{25}\} = T_2 \quad (10)$$

$$\text{Hence, } S: u_{data} = \{ht(s_i), hs(s_j)\} \quad (11)$$

The soft data have the specific PDF,  $f_s$  expressed as:

$$hs(s_j) = \int_{s_j \in T_2} f_s(hs_{soft}) dh_{soft} \quad (12)$$

### Integration (posterior) stage (K)

Modern geostatistics (BME) is not a mere collection of hard data processing techniques unlike classical geostatistics where kriging is a special case. BME estimator depends on the probability law of the spatio or spatiotemporal random field. This stage is associated with the integration and estimation of variables that are highly probable in the light of the specificatory knowledge base being considered. This stage is relative to the total knowledge (posterior),  $K = G \cup S$  (Figure 4): In this last step, the two knowledge bases (G and S) were integrated. The aim is to maximize the posterior PDF given the total knowledge K. BMElab (2014) calculated the posterior PDF at estimation points  $s_k$  using the Bayesian conditionalization rule which was used to update the prior PDF by taking into account the site specific (specificatory) knowledge (i.e., the hard and soft data – and its uncertainty in PDF form and yielded the BME posterior pdf:

$$K = G \cup S \quad (13)$$

Given that the spatial random field,  $u_{map}$

where,

$$u_{map} = (ht_{hard}, hs_{soft}, hp_p) = (u_{data}, hp_p) \quad (14a)$$

and the spatial location:

$$s_{map} = \{s_i, s_j, s_k\} = \{s, s_k\} = T_3 \quad (14b)$$

$$f_k(hp_k(s_k)) = A^{-1} \int_{s_{map} \in T_3} f_s(hs_{soft}) f_G(u_{map}) dh_{soft} \quad (15)$$

where A is the normalization parameter (Christakos, 1990).

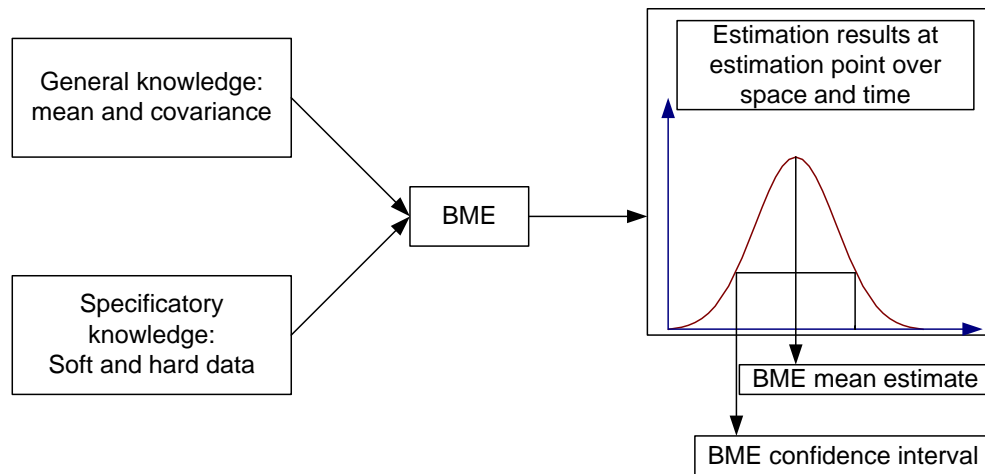


Figure 4. A typical BME mapping process

## Results and Discussion

Figure 5 represents the experimental covariogram (red points) fitted with exponential model (blue line) depicts the spatial continuity structure of the THC hard data. The summary of Figure 5 parameters is shown in Table 1 in terms of the model type, range and the sill such that the range (m) and the sill ( $mg/kg$ ) are 196.85 and 0.88 respectively. The BME prediction map of THC (Figure 6) provides the minimum least square criterion of THC contamination map. Figures 6 shows that the BME prediction lies in the range from 0 to 16  $mg/kg$ , depicting the varying geometry of spread and magnitude of BME prediction in the study area. The extreme western area where the BME prediction (Figure 6) is most concentrated (16  $mg/kg$ ) may likely correspond to point source pollution such as the vandalization of oil-well heads and flowlines, operational failure, surface or underground pipeline leakages due corrosion effect or obsolete equipment, etc., and the concentration decreases from this point to other areas. While some isolated circles in the northern and southern zones of the area do not experience hydrocarbon pollution i.e., has zero (0)  $mg/kg$  BME prediction of THC. Though there are THC guide values for different types of soil, however, the THC guide value for normal soil is 100  $mg/kg$  (Dumitru and Vladimirescu, 2017). Essentially, BME technique offers a realistic representation of the real – world situation which allows the incorporation soft data and its measurement errors. Though indicator kriging (IK) can also incorporate hard data as well as interval data but according to studies conducted by Christakos and Li, 1998, Zhang and Yang, 2019, Rezaei et al., 2020 stated that BME predicts better than IK and asserted that BME did not suffer theoretical and computational shortcomings of IK such as linear estimation and Gaussian probability law. Whereas simple kriging (SK) and ordinary kriging (OK) are special cases of BME that rely solely on hard data under certain restrictive conditions (Christakos and Li, 1998, Christakos, 2000). The BME standard deviation (Figure 7) provides measure of the accuracy assessment of BME prediction map (Figure 6). Such accuracy assessment measure (Figure 7)

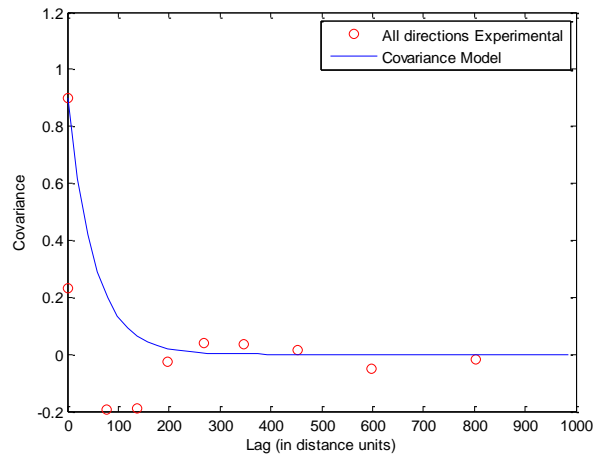


Figure 5. The covariance of the  $THC_{hard}$

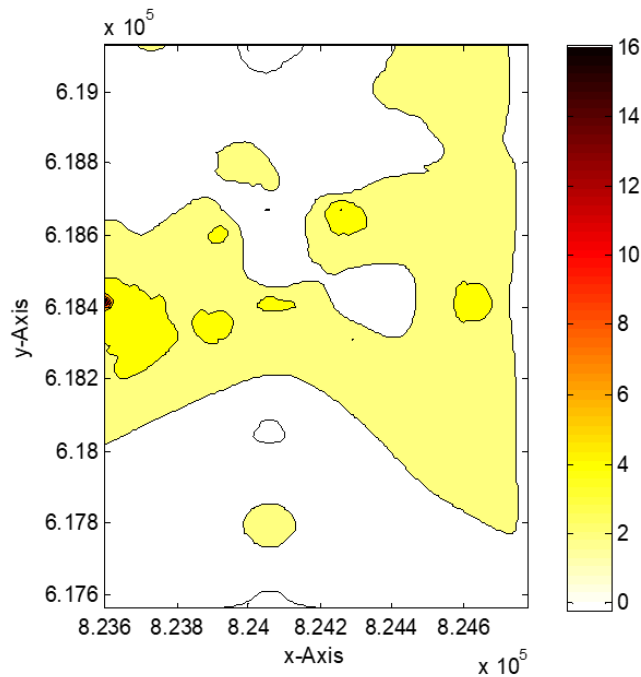


Figure 6. BME Prediction Map of THC ( $mg/kg$ )

is the estimation standard deviation at each location of Figure 6. These values provide a range within which the BME standard deviation map varies from 1 to 8  $mg/kg$ . The BME standard deviation is highest at the region where BME prediction is highest. This result is in agreement with the previous studies that the BME standard deviation depends on the specific set of data considered (Christakos, 2000, Christakos et al., 2004). The high BME estimation standard deviation is attributed to the weak correlation between THC and EC used to

generate the  $THC_{soft}$  and inclusion of its measurement error in the BME prediction of THC.

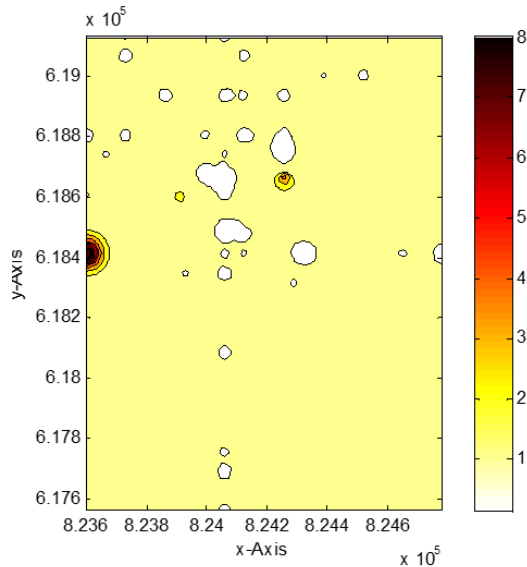


Figure 7. BME standard deviation of THC ( $mg/kg$ )

## Conclusions

This study employed modern geostatistics (i.e., BME) technique to populate and map the spatial variability of THC due to few samples of THC data available amongst the other physico-chemical soil variables sampled. Three datasets assimilated by BME technique are: (i) hard data: 11 THC measurements sampled from the contaminated site, (ii) soft data: these are 28 derived observations from regression model between THC and a covariate (EC), and (iii) 28 uncertainty data of the soft data derived by the probability density function (PDF). The BME technique consists of three interrelated stages – the general knowledge, site specific and data integration stage. BME prediction and BME standard deviation maps of THC were generated. The BME prediction depicts distribution of THC and the magnitude of BME prediction in the study area varies from 0 to 16  $mg/kg$ . The BME prediction where the THC is highest at the western axis of the study area may be due to various reasons such as corrosion effect on the pipelines, activities of saboteur, oil well blow-out due to overpressure, malfunction of equipment just to mention a few. For a normal soil, the guide value for total oil hydrocarbon content in soil is 100  $mg/kg$ . While the BME standard deviation varies between 1 and 8  $mg/kg$ . Moreover, the highest BME standard deviation is at the zone where BME prediction is also the highest which is in accordance with the previous studies that the BME standard deviation rely on the specific set of data used. The results demonstrate the solid theoretical foundation of BME and its computational ability to systematically process soft data coming from regression model and its uncertainty. Therefore, BME is useful for handling and manipulating environmental data where there limited sampled data for reliable

prediction by environmental managers and policy makers so as to make informed decisions.

### **Acknowledgments**

The author thank the GEOTECH, Akure, Nigeria for providing the data to carry out this research and my supervisors at ITC, Enschede, the Netherlands.

### **References**

- Akinlo, A.E. (2012). How important is oil in Nigeria's economic growth? *J Sustain Dev* 5:165–179. doi:10.5539/jsd.v5n4p165
- Awobajo, S. A. (1981). An analysis of oil spill incidents in Nigeria, 1976-1980. In *Proc. Seminar on Petroleum Industry and the Nigeria Environment*, NNPC/FMOW and Housing, P.T.I., Ward, Nigeria.
- BMElab Department of Environmental Sciences and Engineering School of Public Health, University of North Carolina (2014). BMEGUI3.0.1 User Manual. Retrieved from [https://mserre.sph.unc.edu/BMEGUI\\_web/BMEGUI3.0.1\\_web/BMEGUI3.0.1\\_DOCs/PDF/BMEGUI3.0.1\\_UserManual\\_v01.pdf](https://mserre.sph.unc.edu/BMEGUI_web/BMEGUI3.0.1_web/BMEGUI3.0.1_DOCs/PDF/BMEGUI3.0.1_UserManual_v01.pdf)
- Christakos, G. (1990). A Bayesian/maximum-entropy view to the spatial estimation problem. *Math Geol* 22(7):763–777
- Christakos, G. (1992). *Random field models in earth sciences*: Academic Press. San Diego, CA, 474 p
- Christakos, G. (2000). *Modern spatiotemporal geostatistics*. Oxford University Press, New York.
- Christakos, G., & Li, X.Y. (1998) Bayesian maximum entropy analysis and mapping: a farewell to kriging estimators? *Math Geol.*, 30(4):435–462
- Christakos, G., & Serre, M.L. (2000). BME analysis of spatiotemporal particulate matter distributions in North Carolina. *Atmos Environ* 34(20):3393–3406
- Christakos, G., Kolovos, A., Serre, M.L., & Vukovich, F. (2004). Total ozone mapping by integrating databases from remote sensing instruments and empirical models. *IEEE Trans Geosci Remote Sens.*, 42(5):991–1008.
- Cressie, N., & Hawkins, D.M. (1980). Robust estimation of the variogram: I. *J Int Assoc Math Geol.*, 12(2):115–125.
- Douaik, A., Van Meirvenne, M., & Toth, T. (2005). Soil salinity mapping using spatio-temporal kriging and Bayesian maximum entropy with interval soft data. *Geoderma* 128(3–4):234–248.
- Dumitru, M., & Vladimirescu, A. (2017). Loads Limits Values of Soils with Petroleum Hydrocarbons. *Geophysical Research Abstracts*, 19.
- Echefu, N., & Akpofure, E. (2002). Environmental impact assessment in Nigeria: regulatory background and procedural framework. *EIA Train Resour Man*, 63–74.
- Elum, Z.A., Mopipi, K., & Henri-Ukoha, A. (2016). Oil exploitation and its socioeconomic effects on the Niger delta region of Nigeria. *Environ. Sci. Pollut. Res. Int.* 23, 12880-12889. <https://doi.org/10.1007/s11356-016-6864-1>
- Kadafa, A.A. (2012). Oil exploration and spillage in the Niger Delta of Nigeria. *Civ Environ Res* 2(3):31–51

- Kellett, J. (1990). The environmental impact of wind energy developments. *Town Plan Rev* 61:139–155
- Lark, R.M. (2000). A comparison of some robust estimators of the variogram for use in soil survey. *Eur J Soil Sci* 51(1):137–157
- Matheron, G. (1963). Principles of geostatistics. *Econ Geol* 58(8):1246–1266
- Modis K, Vatalis K, Papantonopoulos G, Sachanidis C (2010) Uncertainty management of a hydrogeological data set in a greek lignite basin, using BME. *Stoch Environ Res Risk Assess.*, 24(1):47–56
- Olaseni, M., & Alade, W. (2012). Vision 20:2020 and the challenges of infrastructural development in Nigeria. *J Sustain Dev* 5:63–76. doi:10.5539/jsd.v5n2p63
- Okpokwasili, G.C. & Amanchukwua, S.C. (1988). Petroleum hydrocarbon degradation by *Candida* species. *Environment International*, 14(3):243-247. [https://doi.org/10.1016/0160-4120\(88\)90145-6](https://doi.org/10.1016/0160-4120(88)90145-6)
- Oguine, I. (1999). Nigeria's oil revenues and the oil producing areas. *J Energy Nat Res Law* 2:111–120
- Rezaei, S., Khojasteh, E.R., & Faridazad, M. (2020). Improving geostatistical predictions of two environmental variables using Bayesian maximum entropy in the Sungun mining site. *Stochastic Environmental Research and Risk Assessment*. <https://doi.org/10.1007/s00477-020-01863-4>
- Shi, T.T., Yang, X.M., Christakos, G., Wang, J.F., & Liu, L. (2015). Spatiotemporal interpolation of rainfall by combining BME theory and satellite rainfall estimates. *Atmosphere* 6(9):1307–1326
- Ukhurebor, K.E., Athar, H., Adetunji, C.O., Aigbe, U.O., Onyancha, R.B., & Abifarin, O. (2021). Environmental implications of petroleum spillages in the Niger Delta region of Nigeria: A review. *Journal of Environmental Management*, Volume 293. <https://doi.org/10.1016/j.jenvman.2021.112872>
- Zhang, C.S., Tang, Y., Luo, L., & Xu, W.L. (2009) Outlier identification and visualization for Pb concentrations in urban soils and its implications for identification of potential contaminated land. *Environ Pollut* 157(11):3083–3090.
- Zhang, C., & Yang, Y. (2019). Improving the spatial prediction of soil Zn by converting outliers into soft data for BME method. *Stochastic Environmental Research and Risk Assessment*. <https://doi.org/10.1007/s00477-018-1641-y>
- Suryasa, I. W., Rodríguez-Gámez, M., & Koldoris, T. (2022). Post-pandemic health and its sustainability: Educational situation. *International Journal of Health Sciences*, 6(1), i-v. <https://doi.org/10.53730/ijhs.v6n1.5949>
- Suryasa, I.W., Sudipa, I.N., Puspani, I.A.M., Netra, I.M. (2019). Translation procedure of happy emotion of english into indonesian in kṛṣṇa text. *Journal of Language Teaching and Research*, 10(4), 738–746